Aug 24th, 12:00 AM - Aug 25th, 12:00 AM

Modal Identification of Cold-formed Steel Members in Shell Finite Element Models

Z. Li

S. Ádány

B. W. Schafer

Twenty-First International Specialty Conference on Cold-Formed Steel Structures
St. Louis, Missouri, USA, October 24 & 25, 2012

Modal identification of cold-formed steel members in shell finite element models

Z. Li[1], S. Ádány[2], B. W. Schafer[3]

Abstract

This paper illustrates new capabilities for modal identification of shell Finite Element Method (FEM) models of thin-walled cold-formed steel members. The separation of general deformations into fundamental buckling deformation classes: local, distortional, global, shear, and transverse extension, originated with the constrained Finite Strip Method (*c*FSM) and is extended here to shell element based FEM analysis. The *c*FSM base vectors for general end boundary conditions, previously developed by the authors, provide a series of general base functions capable of separating displacements into classes. FEM displacements are identified by minimizing error between the actual FEM displacements and those predicted by the *c*FSM base functions. This leads to the ability to quantify (i.e., modally identify) the global, distortional, and local participation in a FEM model. The ability to categorize the complicated deformations of a FEM model into simple classes is of great importance because of the different post-buckling and collapse behavior associated with each class. Further, the extension to general FEM models allows for modal identification of members with geometric changes along the length, such as holes, as well as concentrated loads and other characteristics difficult to capture in the finite strip formulation. The method is demonstrated for modal identification of FEM linear elastic analysis, FEM elastic buckling analysis (including highly coupled modes) and FEM nonlinear collapse analysis. Further, the examples include members with holes. The dominance of distortional buckling deformations in collapse regimes of lipped channel members is observed and provides new insight on the interaction of buckling modes in cold-formed steel members. Limitations of the method and future directions for the work are discussed.

Keywords: Modal identification, constrained finite strip method, shell finite element, elastic buckling analysis, collapse analysis

[1] Postdoctoral Fellow, Johns Hopkins Univ., Baltimore, MD, lizhanjie@jhu.edu
[2] Professor, Budapest Univ. of Technology & Economics, sadany@epito.bme.hu
[3] Professor, Johns Hopkins Univ., Baltimore, MD, schafer@jhu.edu

Introduction

Instabilities of cold-formed members, as commonly acknowledged, can be complicated and are generally categorized as: local (local-plate), distortional and global (Euler) buckling. The strength of a member is often governed by these buckling behaviors. The member strength predictions in current design specifications for cold-formed steel [1-3] all employ the elastic buckling loads based on rational analysis either numerical or analytical, then substitute these elastic buckling results into empirical design equations calibrated from experimental or even numerical simulation data to obtain the design strength. However, due to the different post-buckling strength and interactions between buckling modes, appropriate separation and identification of buckling modes are necessary – as currently reflected in design specifications, such as AISI-S100 for cold-formed steel [3]. Moreover, the formulation of empirical design equations, such as in the Direct Strength Method [4] for cold-formed steel member design in AISI [3], is calibrated based on the appropriate categorization of the failure modes into the three buckling mode classes (local, distortional, and global), which is still a process largely relying on subjective visualization and engineering judgment both in experimental tests and numerical simulations.

The popularity and powerful capabilities of the shell Finite Element Method (FEM) in analyzing thin-walled structures, particularly for complex geometry and boundary conditions, make it a natural choice for elastic and nonlinear collapse analyses in many situations. However, FEM itself provides no means of modal identification. A laborious and completely subjective procedure employing visual investigation is required to classify the buckling modes in elastic buckling analysis or categorize the failure mode in nonlinear collapse analysis. Hence, an FEM modal identification method has been proposed for elastic buckling analysis in [5] and nonlinear collapse analysis in [6]. The method originates from the constrained Finite Strip Method (*c*FSM), which has recently been extended to general end boundary conditions, namely: simply-simply (*S*-*S*), clamped-clamped (*C*-*C*), simple-clamped (*S*-*C*), clamped-guided (*C*-*G*), and clamped-free (*C*-*F*) [7]. In *c*FSM, the buckling modes may be decomposed into fundamental deformation classes: global (*G*), distortional (*D*), local (*L*), shear (*S*) and transverse extension (*T*) based on mechanical criteria [7-12]. The base functions in *c*FSM (i.e., the base vectors) are extended to shell FEM degrees of freedom (DOF), and then a minimization problem is solved to calculate the participations of the fundamental deformation classes [13].

In this paper, the modal identification method for shell FEM is briefly summarized and numerical examples are provided for linear elastic analysis, elastic buckling analysis, and nonlinear collapse analysis; including for a member with holes. Limitations and future directions for the work, particularly in integrating the method into the design process, are discussed.

Modal identification methodology based on *c*FSM

The goal of the proposed modal identification is to take an FEM displacement vector (D_{FE}) based on a shell element model of a thin-walled member and accurately assign quantitative modal contributions in terms of the *G*, *D*, *L*, and *ST* classes. For nonlinear collapse analysis on the imperfect structures (i.e., the most general form of the solution) equilibrium in the incremental FEM solution may be expressed as:

$$(K_e + K_g + K_p)\, D_{FE} = F \tag{1}$$

where, K_e is the conventional elastic stiffness matrix, K_g is the geometric stiffness matrix and depends upon the internal forces in the model, K_p is the plastic reduction matrix and accounts for material yielding, and F is the consistent nodal forces. For the special case considering only geometric nonlinearity on the perfect structure an eigen-value problem associated with elastic buckling may be defined as

$$(K_e - \lambda K_g)\, \varphi_{FE} = 0 \tag{2}$$

where, λ is the eigenvalue (load factor), and φ_{FE} is the eigenmode (buckling mode) vector, which is nothing more than a special case of D_{FE}.

The displacement vectors D_{FE} or φ_{FE} are written in terms of the FEM DOF and must be transformed to a basis where the coefficients are participations in DOF associated with *G*, *D*, *L*, and *ST* deformation modes. This is conceptually accomplished through basis R_{FE} that consists of base vectors for the *G*, *D*, *L*, and *ST* deformation modes. An approximation to R_{FE} is utilized based on the *c*FSM basis R_{FS}, this is mathematically convenient because the appropriate basis is already defined for FSM. The solution requires transforming from FSM to FEM space, i.e. extrapolating the *c*FSM displacement vector with 4 DOF for each longitudinal strip term into a displacement vector in shell FEM that has 6 DOF at each node. The extrapolation requires conventional local to global transformations and the shape functions of *c*FSM [7]. The resulting R_{FE}, see details in [14], may then used to determine the modal contribution coefficients by minimizing error between D_{FE} and its approximation $R_{FE}\{c\}$ where $\{c\}$ is a vector of contributions in the *G*, *D*, *L*, and *ST* spaces. Full details regarding the minimization and participation evaluation are provided in [13, 15].

The work herein takes advantage of the generalized FSM longitudinal base function developed in [13]. This set of longitudinal FSM shape functions meets all essential end boundary conditions and consists of the sine series comprising the *S-S* end boundary conditions augmented with the first longitudinal term only (m=1) of the C-F and F-C shape functions, see [7, 13]. The generalized base function is formed using the uncoupled axial modal basis with vector norm in *c*FSM, see [11].

Modal identification for elastic buckling analysis

Elastic buckling analysis with shell FEM (Eq. 2) is performed in the commercial code ABAQUS using the S4 element, a general-purpose shell element [16]. A lipped channel section with the center-line dimensions of Figure 1 is used to illustrate the application and capabilities of the modal identification. The material is assumed to be elastic, isotropic, and homogenous with a Young's modulus of 210000 MPa and Poisson's ratio of 0.3. The member is a column 2000*mm* long with the boundary conditions specified below for each case.

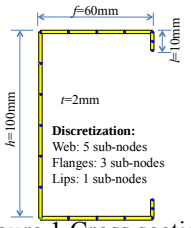

Figure 1 Cross section and mesh

Modal identification of boundary cases in *c*FSM

In FSM general end boundary conditions (i.e., *S-S*, *C-C*, *S-C*, *C-G* and *C-F*) are handled by using specially selected longitudinal shape functions that match the end conditions. Exact matching of the warping end conditions is particularly important. For instance, for *C-F*, the warping, translational and rotational displacements are fixed at the clamped (*C*) end and free (*F*) at the other end. See [13] for detailed fixities for all other cases.

Simulating the FSM end boundary conditions in FEM provides the possibility of a comparison of modal identification between "exact" FSM and "approximate" FEM modal identification based on the FSM generalized base function. Modal identification of five end boundary conditions in both FSM and FEM is shown in Table 1 along with critical loads for the characteristic buckling modes (i.e., *G, D,* and *L*) (Note, the participation results can be extracted from the illustrated example in Figure 2 in the same fashion for all the five cases). Differences are small for both participations and critical loads, highlighting the suitability of the proposed FEM modal identification procedure.

Table 1 Participations and critical loads of FEM and FSM solutions

Boundary case	Charact. mode	Mode number	FEM solution					FSM solution				
			G (%)	D (%)	L (%)	ST (%)	P_{cr} (kN)	G (%)	D (%)	L (%)	ST (%)	P_{cr} (kN)
S-S	**G**	#1	99.4	0.6	0.0	0.0	60.4	99.4	0.6	0.0	0.0	60.6
	D	#3	1.4	95.5	3.1	0.1	160.3	1.3	95.3	3.3	0.1	159.5
	L	#9	0.9	10.3	88.4	0.5	201.5	0.9	6.9	91.8	0.5	191.0
C-C	**G**	#7	93.4	6.4	0.1	0.1	201.6	88.0	11.5	0.3	0.1	201.7
	D	#1	4.7	91.3	3.9	0.1	163.7	2.2	92.3	5.4	0.1	162.3
	L	#5	1.0	7.8	90.7	0.5	201.5	0.9	7.7	91.0	0.5	191.3
S-C	**G**	#1	97.9	2.1	0.0	0.0	112.2	95.3	4.4	0.2	0.1	113.7
	D	#2	2.0	94.1	3.8	0.1	159.1	1.6	93.9	4.4	0.1	157.9
	L	#8	1.2	7.6	90.7	0.5	201.5	0.9	12.4	86.3	0.5	191.1
C-F	**G**	#1	99.7	0.1	0.2	0.0	22.0	99.7	0.1	0.2	0.0	22.1
	D	#7	11.9	82.3	5.6	0.1	163.2	6.0	86.2	7.7	0.1	164.1
	L	#11	1.1	19.8	78.7	0.4	201.5	3.9	12.7	82.9	0.5	191.3
C-G	**G**	#1	99.6	0.4	0.0	0.0	60.6	99.1	0.8	0.0	0.0	60.7
	D	#3	4.7	91.3	3.9	0.1	163.7	3.2	91.3	5.4	0.1	163.2
	L	#7	1.0	7.8	90.7	0.5	201.5	0.9	9.4	89.3	0.5	191.1

Furthermore, as an illustration, participations of *G, D, L,* and *ST* along with critical loads and calculated errors for each mode (50) of the member in Figure 1

with *C*-*F* boundary conditions is provided in Figure 2 (along with selected buckling mode shapes). The participation results are in accordance with engineering expectations. The error is small. The higher modes with non-negligible error are due to the lack of higher longitudinal terms in the base function to account for local buckling with short half-wavelengths. Including more longitudinal terms removes this error (see [13, 15] for more details).

Traditionally, buckling modes are investigated visually, mode-by-mode, and require significant engineering judgment in identification. The *c*FSM based modal identification explored here provides quantitative assessments such as that provided in Figure 2(d) and creates the potential for automating the identification procedure.

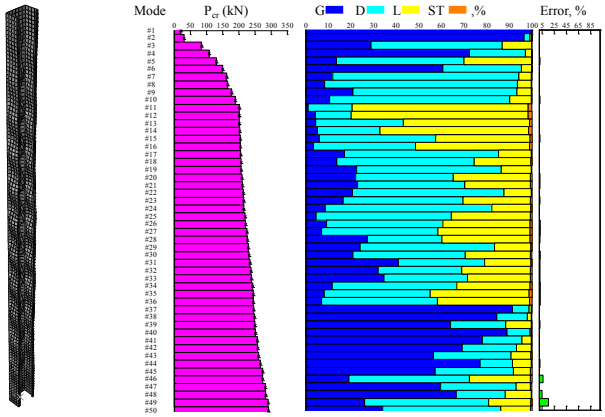

(a) #1 (b) #7 (c) #11 (d) Modal identification

Figure 2 Buckling mode shapes and modal identification of FE solution of *C*-*F*

Arbitrary boundary conditions

In structures, the boundary conditions of a member are in general not simply supported (*S*-*S*) or clamped (*C*-*C*) but rather dependent on the connections and relative member stiffness. For individual members in a structure the boundary conditions may be treated as semi-rigid with appropriate rotational/translational springs employed as illustrated in Figure 3. For the studied member (Figure 1) the semi-rigid end conditions are defined in Figure 3b.

Modal identification of the elastic buckling of the member with semi-rigid end conditions and selected buckling mode shapes are shown in Figure 4. Buckling mode shapes that have translational movements at both ends (1st mode) are found, as shown in Figure 4(a). Quantification of the buckling modes agrees with engineering expectations. Moreover, modal identification for cold-formed steel members in a frame analysis is possible based on this study.

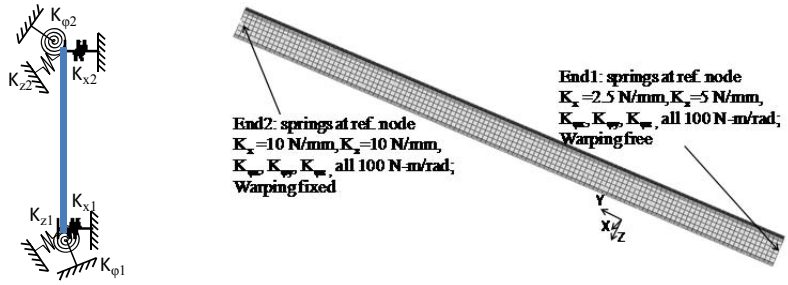

Figure 3 Semi-rigid boundary: a) simplified 2D model; b) boundary conditions and springs in FEM model

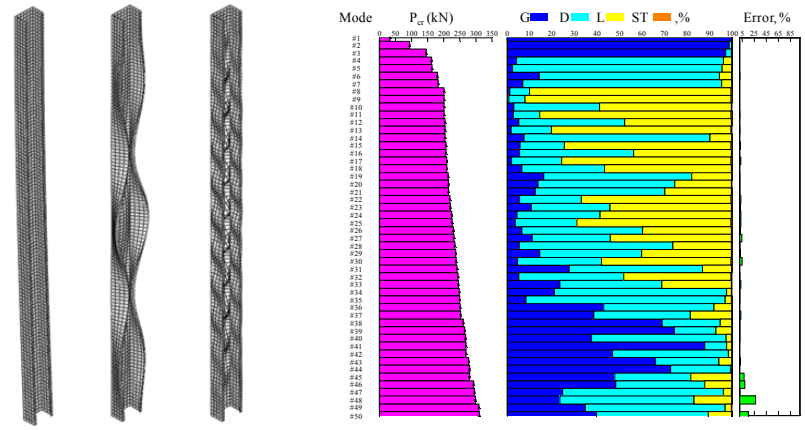

(a) #1 (b) #4 (c) #8 (d) Modal identification

Figure 4 Mode shapes and modal identification of semi-rigid boundary case

Member with holes

Holes are commonly required in cold-formed steel members. The presence of holes can greatly complicate the buckling behavior and modal identification of the member. In FEM laborious visual investigations of the characteristic buckling modes are much more demanding than in member without holes. One apparent barrier is that for members with changes in geometry exact match between the *c*FSM base function and the developed FEM model is impossible. Further, *c*FSM itself is not capable of capturing the changes of section along the length; thus, modal identification using a base function from *c*FSM is a more significant approximation for an FEM model with holes. Nonetheless the procedure works well. Modal identification of the Figure 1 member with holes and boundary conditions as defined in Figure 5 is provided in Figure 6. The error (final column in Figure 6) between φ_{FE} and its approximation $R_{FE}\{c\}$ is small for the studied modes. Further, the indicated participations are in good

agreement with engineering expectations, e.g. see the buckling mode shapes provided in Figure 7. In particular, even with localized deformation shapes around holes as shown in Figure 7(f), the proposed modal identification method captures this deformation with only small error. Moreover, for modes with large global buckling contributions, e.g., the 5th mode of Figures 7(c) and (g), modal identification captures what may not easily be perceived by visualization alone.

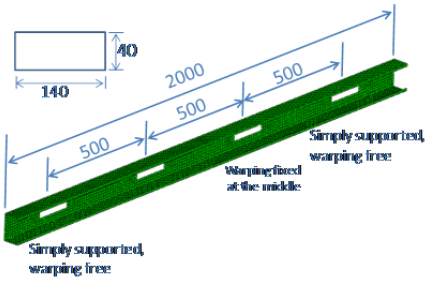

Figure 5 Hole location and size and column boundary conditions (*mm*)

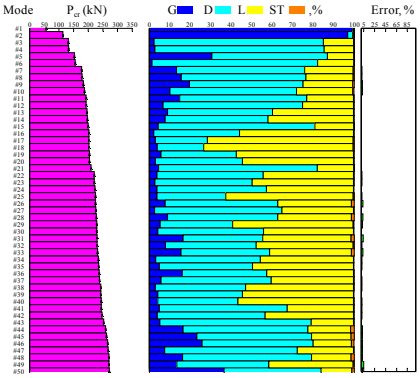

Figure 6 Modal identification of FE solution of member with rect. holes

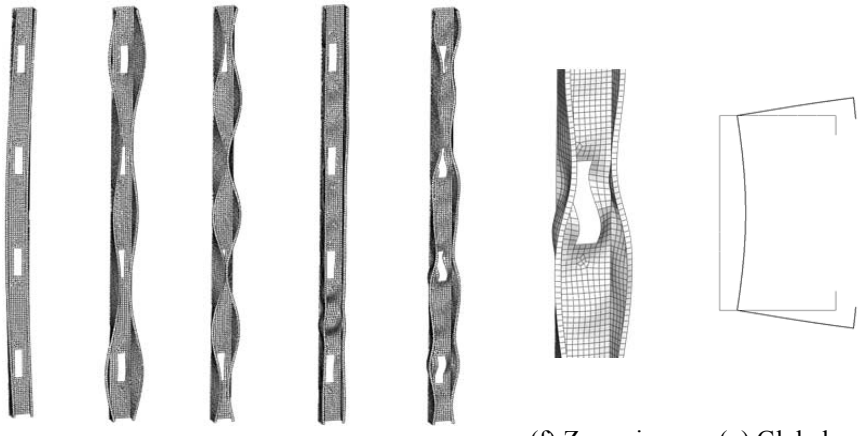

(a) #1 (b) #3 (c) #5 (d) #17 (e) #22 (f) Zoom-in near hole #22 (g) Global feature in #5

Figure 7 Selected buckling mode shapes for member with holes

Modal identification for linear elastic static analysis

Before delving into the more complicated cases, a simpler problem – modal identification of a linear static analysis is considered. This is a simplified version of Eq. (1) with K_g=K_p=0 and no updating of K_e. Modal identification is performed on the displacement vector D_{FE}. In this particular study, a special set of linear elastic static analyses is performed. According to *c*FSM, for the global and distortional buckling modes the deformation can be solely determined once the warping displacement V is known (see [7, 9] for relations of other displacements to *V)*. Two warping distributions that correspond to major-axis bending and symmetric distortional buckling are prescribed on a lipped channel section in Figure 1 for linear static analysis (see details in [14]).

The deformed shape (D_{FE}) shown in Figure 8 and 9 are generated from linear elastic static analysis by prescribing the V displacements of major-axis bending and symmetric distortional buckling along the member with *S*-*S* and *C*-*C* boundary conditions, respectively (see details in [14]). The number of half - waves along the length is 1 for major-axis bending, and for distortional buckling is 6 for *S*-*S* and multiple participating half-waves for *C*-*C* [13, 14]. In Figure 8, the deformations are in major-axis bending, as commonly acknowledged, and the modal identification indicates 99.9% G participation. In Figure 9 the deformations are clearly distortional in nature and the modal identification indicates 98% D and 2% L participation.

Modal identification of the linear elastic static analysis in this section demonstrates the veracity of the mechanical assumptions in [7-12] regarding global and distortional buckling as well as demonstrates the applicability of FEM modal identification on a general displacement vector, i.e. D_{FE}.

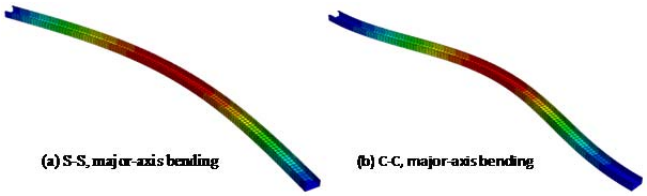

Figure 8 Deformed shapes of major-axis bending for S-S and C-C

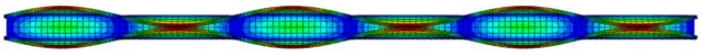

(a) S-S, symmetric distortional with longitudinal term m=6

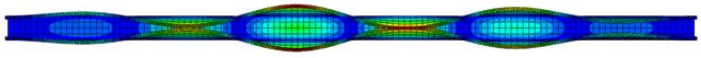

(b) C-C, symmetric distortional with multiple longitudinal terms

Figure 9 Deformed shapes of symmetric distortional for S-S and C-C

Modal identification for nonlinear analysis

In this section, modal identification for two kinds of shell FEM nonlinear analyses are studied: 1) elastic post-buckling analysis, i.e. a nonlinear analysis with only geometric nonlinearity (K_p=0 in Eq. (1)); and 2) nonlinear collapse analysis, i.e. a nonlinear analysis with both geometric and material nonlinearity. The numerical examples provide modal identification results for pre-buckling, post-buckling, and collapse mechanisms.

For incremental nonlinear analysis on the imperfect member the displacement vector to be identified D_{FE} must be considered with care. The *c*FSM basis, R_{FS}, which is transformed to R_{FE} and utilized for the modal identification process is based on the perfect geometry, but in nonlinear collapse analysis the deformation vector D_{FE} is based on a model of the member with initial geometric imperfections. Consequently, identification is instead performed on:

$$D_{FEid} = D_{FE} + D_{imp} \tag{3}$$

where, D_{FEid} is the deformation vector to be identified in terms of *G, D, L,* and *ST*, and D_{imp} is the imperfection deviating from the perfect model. This is consistent with the *c*FSM basis and only influences the solution for small D_{FE}.

Member and modeling

The cold-formed steel member used for illustration (termed the local dominated member) is again a channel section similar to Figure 1, but now with: *f=50.8mm, h=152.5mm, l=15.9mm,* and *t= 1.1455mm.* The member is modeled as a *600mm* long column with local-plate simply supported end conditions, i.e., pinned at all nodes at the member ends. The mesh density in the web is doubled from that of Figure 1. The material is the same as before except modeled as elastic-perfectly plastic (von Mises yield criteria with isotropic hardening) with a yield stress of 345 MPa. The member is specially chosen to be dominated by local buckling as indicated from eigen-buckling analysis: where modal participations in the first mode are 95% *L* and 4.8% *D* and the critical buckling load is 20.8 *kN*.

Shell FEM modeling of thin-walled members is highly sensitive to model inputs such as geometric imperfections, residual stresses, plastic strain, yield criteria, material model, boundary conditions, and also the fundamental mechanics particularly with regard to element selection and solution schemes [17, 18]. Details about geometric imperfections are provided below and in [6, 14]. The analyses performed herein utilize the commercial finite element ABAQUS [16] using the arc-length method solver (modified Riks method [19]).

Ultimate strength and developed failure mechanisms are both imperfection sensitive; therefore, careful treatment of geometric imperfections is of significant importance in modeling thin-walled members. Both the imperfection

distribution and magnitude must be considered. Here, for modeling convenience, the distribution of the imperfections are seeded from the local or distortional mode shapes generated from a CUFSM analysis with *S*-*S* boundary conditions [11], and the magnitude is a function of the member's thickness *t*, as provided in Table 2. It is worth noting here that if one wants to simulate tests or provide strength predictions of cold-formed steel members in a more reliable and accurate manner, the distribution and magnitude of imperfections should be more closely tied to measured data [17, 18].

Table 2 Imperfection cases and their peak loads

Case	Waves along member	Distribution	Magnitude	Peak load (kN)
I	n/a	n/a	0	72.9
II	5	Local	0.1t	72.1
III	1	Outward distortional	0.1t	73.1
IV	1	Inward distortional	0.1t	72.6
V	1	Outward distortional	0.94t	68.3

Linear elastic deformation in modal identification

In elastic post-buckling analysis and full nonlinear collapse analysis D_{FE} is based on incremental response and includes primary deformations due to the applied loading and additional deformations potentially sympathetic with the buckling modes. The modal identification of these additional deformations is of primary interest in thin-walled members. Thus, the buckling behavior of the member in nonlinear analysis is made clearer when this direct linear elastic response is removed (see [14]):

$$D_{\varphi}=D_{FE}+D_{imp}-D_{LE} \quad (4)$$

where D_{LE} is the linear elastic deformation under the applied load and D_{φ} is the displacement vector to be identified. In the simplest loading cases (compression, bending, etc.) D_{LE} is coincident with a global deformation mode. For the column studies here D_{LE} is coincident with G4 as shown in Figure 10(e). For the following numerical examples, modal identification results on D_{φ} (as opposed to D_{FEid}) are provided and termed as the *adjusted* participations, as illustrated in Figure 10(f)-(j).

Modal identification: linear post-bucking and collapse analyses

Elastic post-buckling and collapse analyses are performed for the imperfection cases provided in Table 2. Figure 10(a) provides the load-displacement responses for both the elastic post-buckling and nonlinear collapse analyses of the local dominated member. Key deformed shapes of the member are provided in Figure 10(b)-(d). Eigen-buckling analysis shows that the elastic local buckling load is 21 kN. Nonlinear collapse analysis provides a peak strength of approximately 73 kN. This member has remarkable post-buckling reserve.

First, the local dominated member shows only mild imperfection sensitivity as indicated in Figure 10(a). The strength of the member is not greatly influenced by a small amount of imperfections (case II-IV), but is significantly reduced when the magnitude is bigger (case V). Further, peak loads provide in Table 2 illustrate that not all imperfections are detrimental: at small magnitudes the outward distortional imperfection (case III) actually increases the strength above the no imperfection result (case I).

Second, elastic post-buckling and collapse analyses demonstrate the importance of distortional (*D*) deformation in the final post-buckling and post-peak collapse regimes no matter what magnitudes and distributions of imperfections are prescribed in the models and also independent of the material nonlinearity, as shown in Figure 10(e)-(h). This is consistent with experimental observations in [20]. Material nonlinearity triggers a dramatic transition between *L* and *D* deformations and localization of the response. Due the material plasticity, the post-peak collapse mechanism is formed earlier and rapidly as shown in Figure 10(f)-(j) and also results in a more localized deformation than the elastic post-buckling case, as provided in Figure 10(d) and (c), respectively.

Third, imperfection magnitude and distribution can radically alter idnetified pre-peak deformations and the peak failure mode, but in the end the same post-peak collapse behavior is triggered. Modal participations in Figure 10(g)-(j) indicate that the deformation mode is in accordance with the applied imperfection in the pre-buckling stage, but the model buckles into the local mode (case II-IV) or interacted mode (case V) depending on the magnitude of imperfection. The models also demonstrate that a locally dominant member indeed fails as a local mode at the peak for no (case I) or small imperfection (case II-IV) in Figure 10(e)-(i), but otherwise leads to a local-distortional interacted mode for large imperfections (case V) as in Figure 10(j). However, in the post-peak collapse regime the distortional mode dominates the deformation. Furthermore, imperfection model III and IV further illustrate that the inward and outward distortional imperfection trigger different responses.

Fourth, shear and transverse deformations (*ST*), which are not obvious in eigen-buckling modes, have growing importance in the post-buckling/post-peak collapse regimes. *ST* modes in these regimes typically have greater than 2% of the participation, which is consistent with observations in Generalized Beam Theory [21]. Also, for the no imperfection model of Figure 10(e), the initial deformations (primarily associated with localized deformations due to the end boundary conditions) have a noticeable *ST* contribution.

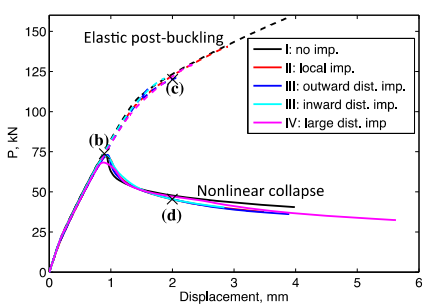

(a) Load-disp. responses (scale: 2)

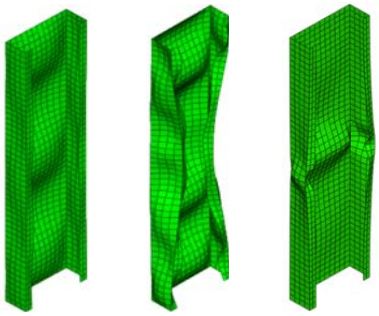

(b) peak (c) 2 mm (d) 2 mm

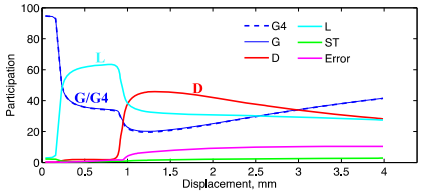

(e) I: no imperfection with G4

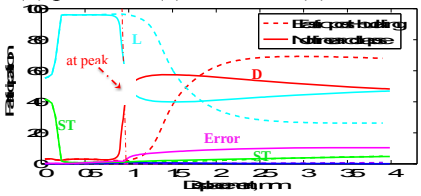

(f) I: no imperfection

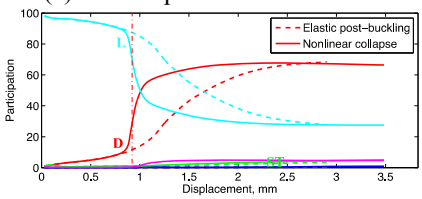

(g) II: local imperfection (0.1t)

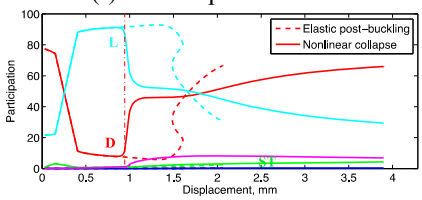

(h) III: outward dist. Imp. (0.1t)

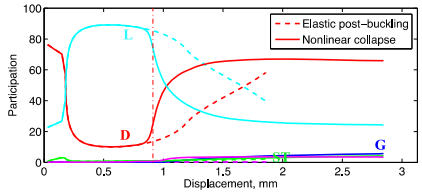

(i) IV: inward dist. Imp. (0.1t)

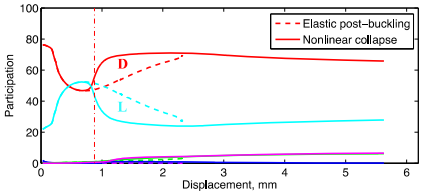

(j) V: large dist. Imp. (0.94t)

Figure 10 Nonlinear analyses of the local dominated models

Finally, it is worth noting that the error in the identification process is normally larger in the collapse regime due to the localization of the deformations, while it is small in its counterpart elastic post-buckling analysis. Potentially, including *c*FSM base vectors with a larger number of longitudinal terms can reduce this error. However, the additional computational effort would be significant.

Discussion

The examples provided herein are all for columns. Application to bending or other more general loading cases are possible, as demonstrated in [13] for eigen-buckling analysis of a partially restrained beam. Modal identification of the nonlinear collapse analysis for other models can also be found in [14]. However, for nonlinear collapse analysis, a key issue that arises in the analysis that requires further study is how to handle the primary displacement associated with a given loading. The proposed solution here (D_φ) still needs further investigation for more complicated loading patterns.

The collapse analyses of perfect models suggest the member fails at peak as the eigenmode predicts. However, studies of the imperfect models show that the failure mode also relies on the prescribed imperfections. Moreover, from a behavioral standpoint the dominance of distortional buckling in the post-buckling/collapse regime of lipped channels, independent of the pre-buckling or pre-peak deformations is an interesting result. The collapse mechanisms are typically better captured by the distortional modes. Plasticity only triggers the development of this stable distortional mode in collapse regime earlier sand may also bring other modes in due to localization. Moreover, when material nonlinearity is present this extension of the elastic FSM base vectors to describe plastic deformation fields is practical, and appears potentially useful in an engineering sense, but further work is needed before such identification could be considered rigorous.

Significant future work remains to advance the modal identification method presented here. For example, integration of the quantitative modal participation results into design methods has great potential, particularly for members with highly interacted modes. Another area of potential includes connecting the collapse mechanisms and their related energy dissipation to the *G, D, L,* and *ST* deformation spaces. This could be useful for developing simple design methods that characterize energy dissipation in members as currently no simple means exists for this much needed quantity.

Conclusions

Modal identification for thin-walled members, developed in the context of the constrained Finite Strip Method, is extended to finite element models of thin-walled members meshed with shell elements. The developed method is able to identify and quantify the global, distortional, local, shear, and transverse extension modal participations for linear elastic analysis, eigen-buckling analysis, elastic post-buckling analysis, and full nonlinear collapse analysis conducted on shell element-based finite element models of thin-walled members. The identification method is shown to provide meaningful results even when the finite element model has irregularities that cannot be directly captured in the

finite strip method such as holes or partially restrained end boundary conditions. Modal identification of a cold-formed steel lipped channel under compression for eigen-buckling, elastic post-buckling, and nonlinear collapse analysis demonstrates the nature of the available results and provides new insights on the behavior of cold-formed steel lipped channel members. With the developed method it is possible to examine how participation, for example in the local mode, evolves under load. For the studied lipped channel, which has a first mode clearly controlled by local buckling the analyses reveal the importance of the distortional mode in post-buckling and its dominance in characterizing the response in collapse. The role of other modes is also provided in the modal identification results, for example, the model shows how shear and transverse extension modes play a small but growing role in the collapse regime. Future work remains to further develop this new technique, and to extend its applicability in design.

Acknowledgement
This paper is based in part upon work supported by the U.S. National Science Foundation under Grant No. 0448707. Any opinions, findings, and conclusions or recommendations expressed in this material are those of the author(s) and do not necessarily reflect the views of the National Science Foundation.

References

1. *Eurocode 3: design of steel structures, part 1.3: general rules. ENV 1993-1-3*, 1996, European Committee for Standardisation (CEN).
2. AS/NZS, *Cold-formed steel structures, AS/NZS 4600*, 1996, Standards Australia/Standards New Zealand.
3. NAS, *2007 Edition of the North American Specification for the Design of Cold-Formed Steel Structural Members*2007, Washington, DC: American Iron and Steel Institute.
4. AISI, *Direct Strength Method Design Guide*2006, Washington, DC.
5. Li, Z., et al. *Modal identification for finite element models of thin-walled members.* in *Proceedings of the 6th Intl. Conf. on Thin-Walled Structures*. 2011. Timisoara, Romania.
6. Li, Z., et al., *Modal identification in nonlinear collapse analysis of thin-walled members*, in *Structural Stability Research Council Annual Stability Conference* 2011: Pittsburg, PA. p. pp. 168-180.
7. Li, Z. and B.W. Schafer. *Finite Strip Stability Solutions for General Boundary Conditions and the Extension of the Constrained Finite Strip Method*. in *Trends in Civil and Structural Engineering Computing*. 2009. Stirlingshire, UK: Saxe-Coburg Publications.

8. Ádány, S. and B.W. Schafer, *Buckling mode decomposition of single-branched open cross-section members via finite strip method: Derivation.* Thin-Walled Structures, 2006. **44**(5): p. 563-584.
9. Ádány, S. and B.W. Schafer, *A full modal decomposition of thin-walled, single-branched open cross-section members via the constrained finite strip method.* Journal of Constructional Steel Research, 2008. **64**(1): p. 12-29.
10. Li, Z. and B.W. Schafer, *The constrained finite strip method for general end boundary conditions.*, in *Structural Stability Research Council - Proceedings of the 2010 Annual Stability Conference*2010: Orlando, FL, USA. p. 573-591.
11. Li, Z. and B.W. Schafer. *Buckling analysis of cold-formed steel members with general boundary conditions using CUFSM: Conventional and constrained finite strip methods*. in *20th International Specialty Conference on Cold-Formed Steel Structures: Recent Research and Developments in Cold-Formed Steel Design and Construction*. 2010. St Louis, MO.
12. Schafer, B.W. and S. Ádány, *Buckling analysis of cold-formed steel members using CUFSM: Conventional and constrained finite strip methods.*, in *Eighteenth International Specialty Conference on Cold-Formed Steel Structures: Recent Research and Developments in Cold-Formed Steel Design and Construction,* 2006. p. 39-54.
13. Li, Z., *Finite strip modeling of thin-walled members*, in *Departement of Civil Engineering*2011, Johns Hopkins University: Baltimore. p. 240.
14. Li, Z., S. Ádány, and B.W. Schafer, *Modal identification of thin-walled members in nonlinear collapse analysis by shell finite elements.* Thin-Walled Structures, 2012.
15. Ádány, S., A.L. Joó, and B.W. Schafer, *Buckling mode identification of thin-walled members by using cFSM base functions.* Thin-Walled Structures, 2010. **48**(10-11): p. 806-817.
16. ABAQUS, *ABAQUS theory manual (v6.7)*, 2007, ABAQUS, Inc.
17. Schafer, B.W., Z. Li, and C.D. Moen, *Computational modeling of cold-formed steel.* Thin-Walled Structures, 2010. **48**(10-11): p. 752-762.
18. Schafer, B.W. and T. Peköz, *Computational modeling of cold-formed steel: Characterizing geometric imperfections and residual stresses.* Journal of Constructional Steel Research, 1998. **47**(3): p. 193-210.
19. Crisfield, M.A., *A fast incremental/iterative solution procedure that handles "snap-through".* Computers & Structures, 1981. **13**(1-3): p. 55-62.
20. Yu, C. and B.W. Schafer, *Local buckling tests on cold-formed steel beams.* Journal of Structural Engineering, 2003. **129**(12): p. 1596-1606.
21. Silvestre, N. and D. Camotim, *Non-linear generalised beam theory for cold-formed steel members.* International Journal of Structural Stability and Dynamics, 2003. **3**(4): p. 461-490.